

# Direct measurements of heterobarrier leakage current and modal gain in 2.3 μm double QW p-substrate InGaAsSb/AlGaAsSb broad area lasers

D.V. Donetsky, G.L. Belenky, D.Z. Garbuzov, H. Lee, R.U. Martinelli, G. Taylor, S. Luryi and J.C. Connolly

The heterobarrier hole leakage current and modal gain for GaSb-based lasers have been measured for the first time. It is shown that this leakage current is not a factor limiting high temperature operation of the device. Significant broadening of the optical gain with increasing temperature is demonstrated.

Recent success in the design of broadened waveguide lasers [1] has made possible the operation of mid-infrared GaSb-based lasers above room temperature due to a reduction of internal loss. Measurements of temperature dependencies of heterobarrier leakage and modal gain are essential for a better understanding of the role of different phenomena determining the device temperature performance.

To measure the heterobarrier leakage current of holes in 2.3 μm InGaAsSb/AlGaAsSb lasers, we designed and fabricated broad area devices on p-substrates. Essentially, we have grown an n-p-p<sup>+</sup> hole collector on the top of a laser structure. The inset in Fig. 1 shows schematically the band diagram of the laser with the collector under bias. The holes emitted from the active region into the n-cladding layer were collected by a small reverse biased pn junction on the top of n-cladding. The saturation current of the collector directly reflects the carrier leakage. This technique was previously applied to InP-based lasers to measure the leakage of electrons [2].

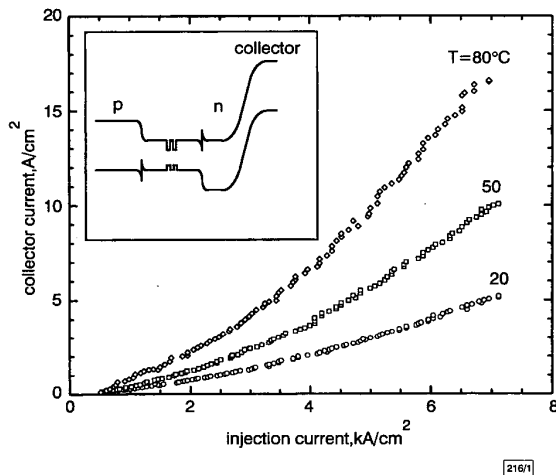


Fig. 1 Dependence of heterobarrier hole leakage current on injection current for different temperatures

Inset: schematic laser band diagram with built-in hole collector

The active region of studied lasers has a structure similar to that described in [3] and consists of two strained quantum wells (QWs). Distinctive features of the lasers used in the present work are the p-substrate and a small collector on the top of the n-cladding. To fabricate the collector, we have developed, for the first time, a self-aligned technique for GaSb. As a wet etch, we used either photoresist developer or citric acid mixed in a 10 : 1 ratio with hydrogen peroxide. We grew two similar 2.3 μm InGaAsSb/AlGaAsSb broadened waveguide laser heterostructures with slightly different n-cladding designs by molecular beam epitaxy on GaSb substrates. The heterostructures have the following sequence of layers. The p-cladding with Al<sub>0.9</sub>Ga<sub>0.1</sub>As<sub>0.625</sub>Sb<sub>0.375</sub> composition is doped to 10<sup>18</sup> cm<sup>-3</sup>. The active region containing two QWs is surrounded by two 0.34 μm undoped Al<sub>0.31</sub>Ga<sub>0.69</sub>As<sub>0.625</sub>Sb<sub>0.375</sub> separate confinement layers (SCH). The n-cladding layer with doping of 2–3 × 10<sup>17</sup> cm<sup>-3</sup> and composition Al<sub>0.5</sub>Ga<sub>0.5</sub>As<sub>0.625</sub>Sb<sub>0.375</sub> has a width of 2 μm. The first structure, ITV923, has an Al<sub>0.9</sub>Ga<sub>0.1</sub>As<sub>0.625</sub>Sb<sub>0.375</sub> layer of 20 nm width incorporated between the SCH and the n-cladding. The second structure ITV926 was grown without this

layer. The hole collector contains n-p-p<sup>+</sup> GaSb layers. The collector area of 5 × 10 μm<sup>2</sup> does not exceed 1% of the current-injection area 10 × 500 μm<sup>2</sup>. The collection efficiency of holes is better than 50% since the hole recombination in indirect n-cladding is insignificant. Fig. 1 shows the dependencies of collector current on injection current for the structure ITV923. The results are similar for the structure ITV926. It can be seen that the measured hole leakage current does not exceed 0.5% of the injection current, over the whole range of measured currents and temperatures. Hence, the hole heterobarrier leakage current should not be a limiting factor for high temperature operation of 2.3 μm InGaAsSb/AlGaAsSb lasers.

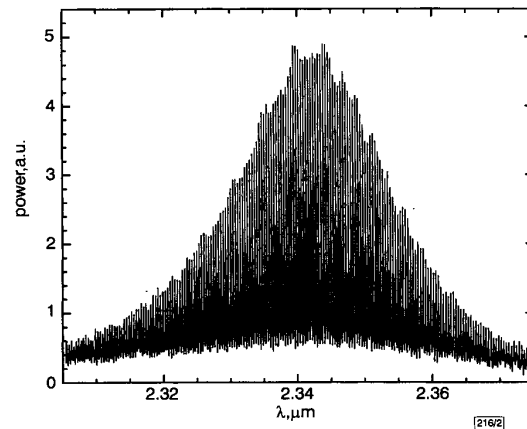


Fig. 2 Amplified spontaneous emission spectrum measured with Fourier-transform spectrometer

Resolution: 0.125 cm<sup>-1</sup>

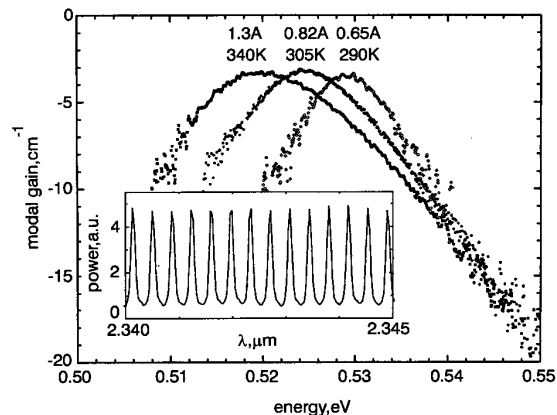


Fig. 3 Modal gain spectra for different temperatures

Inset: portion of amplified spontaneous emission spectrum

The modal gain measurements were made on broad area lasers using Hakki-Paoli technique [4]. We fabricated 100 μm × 2 mm broad area lasers with high reflection and neutral mirror coatings from the ITV923 structure without a collector. The lasers were thermally stabilised and operated in the pulsed-current regime to prevent overheating. The amplified spontaneous emission (ASE) spectra (Fig. 2) were measured using a Fourier-transform spectrometer Nicolet Magna-860 with resolution as high as 0.125 cm<sup>-1</sup>. A spatial filter was used to filter out all but the on-axis emission. It should be noted that a Michelson interferometer itself acts as an effective mode selector, because only the on-axis mode contributes to the interferogram. The modal gain spectra were extracted using the following expression [4]:

$$g = -\frac{1}{L} \ln \left( \frac{\sqrt{P_{max}/P_{min}} + 1}{\sqrt{P_{max}/P_{min}} - 1} \right)$$

where  $g$  is the modal gain,  $L$  is the cavity length,  $P_{max}$  and  $P_{min}$  are the intensities of maxima and minima of the ASE spectra. The measured modal gain spectra for different temperatures are

presented in Fig. 3. The injection current values are close to the corresponding lasing threshold currents for each temperature. The inset in Fig. 3 shows a part of the ASE spectrum. We discovered a substantial broadening of the gain spectra with increasing temperature. Assuming the internal loss to be  $2\text{cm}^{-1}$  [1], we can estimate the total loss (internal plus mirror output) as  $4.5\text{cm}^{-1}$ . In this case, the full-width half-maximum of material gain at room temperature is  $\sim 10\text{meV}$  and increases at least by a factor of 2 at  $T = 340\text{K}$ . The observed rate of gain broadening is more noticeable than the corresponding rate reported for  $1.3\mu\text{m}$  InGaAsP lasers [5].

In conclusion, we have measured the temperature dependencies of the heterobarrier leakage current of holes and of the optical gain in  $2.3\mu\text{m}$  QW InGaAsSb/AlGaAsSb lasers for the first time. It has been shown that the hole heterobarrier leakage current is not a limiting factor on high temperature operation of the device. We discovered an essential broadening of the gain spectra in  $2.3\mu\text{m}$  QW InGaAsSb/AlGaAsSb lasers with temperature. This broadening and the associated laser gain suppression can be essential factors of the device temperature performance.

**Acknowledgments:** This work was supported by Air Force Office of Scientific Research under grant #F-49620-98-1-0133.

© IEE 1999

3 December 1998

Electronics Letters Online No. 19990242

DOI: 10.1049/el:19990242

D.V. Donetsky, G.L. Belenky and S. Luryi (State University of New York at Stony Brook, NY 11794, USA)

D.Z. Garbuzov, H. Lee, R.U. Martinelli, G. Taylor and J.C. Connolly (Sarnoff Corporation, 201 Washington Rd, Princeton, NJ 08543, USA)

## References

- GARBUZOV, D.Z., MARTINELLI, R.U., LEE, H., YORK, P.K., MENNA, R.J., CONNOLLY, J.C., and NARAYAN, S.Y.: 'Ultralow-loss broadened-waveguide high-power  $2\mu\text{m}$  AlGaAsSb/InGaAsSb/GaSb separate-confinement quantum-well lasers', *Appl. Phys. Lett.*, 1996, **69**, (14), pp. 2006–2008
- BELENKY, G.L., KAZARINOV, R.F., LOPATA, J., LURYI, S., TANBUN-EK, T., and GARBINSKI, P.A.: 'Direct measurements of the carrier leakage out of the active region in InGaAsP/InP laser heterostructures', *IEEE Trans.*, 1995, **42**, (2), pp. 215–218
- GARBUZOV, D.Z., LEE, R., KHALFIN, V., DIMARCO, L., MARTINELLI, R., MENNA, R., and CONNOLLY, J.C.: '2.3–2.6  $\mu\text{m}$  CW high-power room temperature broaden waveguide SCH-QW InGaAsSb/AlGaAsSb diode lasers'. CLEO-98, San Francisco, May 1998 (Postdeadline papers)
- HAKKI, B.W., and PAOLI, T.L.: 'CW degradation at 300 K of GaAs double-heterostructure junction lasers. II. Electronic gain', *J. Appl. Phys.*, 1973, **44**, pp. 4113–4119
- ACKERMAN, D.A., SHTEINGEL, G.E., HYBERTSEN, M.S., MORTON, P.A., KAZARINOV, R.F., TANBUN-EK, T., and LOGAN, R.A.: 'Analysis of gain in determining of To in  $1.3\mu\text{m}$  semiconductor lasers', *IEEE J. Sel. Topics Quantum Electron.*, 1995, **1**, (2), pp. 250–263

## Dynamic noise responses of DFB fibre lasers in presence of pump power fluctuations

Y. Qian, P. Varming, J.H. Povlsen and V.C. Lauridsen

A model is presented for relative intensity noise (RIN) in DFB fibre lasers which predicts the measured characteristics accurately. Calculation results imply that the RIN decreases rapidly with a stronger Bragg grating and higher pump power.

**Introduction:** To improve the stability of DFB fibre lasers [1] it is important to understand their dynamic behaviour in the presence of pump power fluctuations. The laser design can then be optimised to suppress relaxation oscillations around the peak of the RIN spectrum. Previously, relaxation oscillations in F-P fibre lasers have been analysed using two coupled rate equations [2]. This approach is not appropriate for DFB fibre lasers due to the presence of strong spatial hole-burning similar to that in semiconductor DFB lasers [3]. The dynamic behaviour of semiconductor DFB lasers has been studied using complex models such as the

CLADISS [4] model, which combines coupled-mode theory with the rate equations. We propose here for the first time a simplified model based on three spatially-independent rate equations to describe the dynamic response of erbium doped DFB fibre lasers in the presence of pump power fluctuations, using coupled-mode theory to calculate the steady-state hole-burning profile of the erbium-ion inversion.

**Model and equations:** The conventional rate equations for inversion  $x(z, t)$ , forward and backward signal photon currents  $n_s^+(z, t)$  and  $n_s^-(z, t)$  can be described as

$$\frac{\partial x(z, t)}{\partial t} = (\Gamma_s \sigma_{g,s} n_s + \Gamma_p \sigma_{g,p} n_p) - \frac{x(z, t)}{\tau_{21}} \equiv F(z, t) \quad (1)$$

$$\frac{n_{eff}}{c} \frac{\partial n_s^\pm(z, t)}{\partial t} = -\Gamma_s \sigma_{g,s} n_s^\pm(z, t) \rho \mp \frac{\partial n_s^\pm(z, t)}{\partial z} \quad (2)$$

$$n_r = \frac{p_r}{h\nu_r A_{eff}} \quad \sigma_{g,r} = (1-x)\sigma_{a,r} - x\sigma_{e,r} \quad (r = s, p)$$

where  $s$  and  $p$  refer to the signal and pump,  $a$  and  $e$  to absorption and emission, and  $g$  to gain.  $n_s = n_s^+ + n_s^-$  the total signal photon current, and  $p$  the power. Parameters  $\sigma$  and  $\rho$  refer to the  $\text{Er}^{3+}$  cross-section and concentration, respectively,  $\Gamma$  the confinement factor,  $h\nu$  the photon energy,  $\tau_{21}$  the laser upper-level lifetime and  $A_{eff}$  and  $n_{eff}$  the effective area and refractive index of the fibre core, respectively. Constant  $c$  is the speed of light.

The spatial distributions of the inversion, signal and pump photon currents are described using the envelope functions  $f_s$ ,  $f_s$  and  $f_p$ , respectively, while the temporal variations of the inversion and photon current are expressed by  $\alpha$  and  $\epsilon$ , respectively:

$$x(z, t) = x(z) + \alpha_s(t)x_s(z) + \alpha_p(t)x_p(z) \quad (3)$$

$$n_r(z, t) = n_{r0}(1 + \epsilon_r(t))f_r(z) \quad (r = s, p) \quad (4)$$

$$x_r(z) = n_{r0} \frac{\partial x(z)}{\partial n_{r0}} \quad x(z) = x_0 f_x(z) \quad (r = s, p)$$

The envelope functions  $f_s$ ,  $f_s$  and  $f_p$  the average photon currents  $n_{s0}$  and  $n_{p0}$ , and the average inversion  $x_0$  are calculated from steady-state coupled-mode theory [5].

By substituting model eqns. 3 and 4 into eqns. 1 and 2 and integrating them over the entire cavity length  $L$  with the integral notation  $\langle f \rangle = \int_0^L f(z, t) dz / L$  and normalisation  $\langle f_s \rangle = \langle f_s \rangle = \langle f_p \rangle \equiv 1$ , we obtain the new simplified and spatially-independent rate equations

$$\frac{d\alpha_s(t)}{dt} = \frac{\langle F \cdot x_s \rangle \cdot \langle x_p^2 \rangle - \langle F \cdot x_p \rangle \cdot \langle x_s \cdot x_p \rangle}{\langle x_p^2 \rangle \cdot \langle x_s^2 \rangle - \langle x_p \cdot x_s \rangle^2} \quad (5)$$

$$\frac{d\alpha_p(t)}{dt} = \frac{\langle F \cdot x_p \rangle \cdot \langle x_s^2 \rangle - \langle F \cdot x_s \rangle \cdot \langle x_s \cdot x_p \rangle}{\langle x_p^2 \rangle \cdot \langle x_s^2 \rangle - \langle x_p \cdot x_s \rangle^2} \quad (6)$$

$$\frac{d\epsilon_s(t)}{dt} = \frac{c(1 + \epsilon_s)}{n_{eff}} \left( \frac{f_s(0) + f_s(L)}{L} + \Gamma_s \rho \langle \sigma_{g,s} \cdot f_s \rangle \right) \quad (7)$$

Eqns. 5–7 can be used to describe the dynamic responses to pump power fluctuations. Using Fourier transformation, the laser noise characteristics can also be analysed. We define the relative intensity noise as  $RIN_{laser} = \langle \Delta p_s^2 \rangle / p_{s0}^2$  ( $\text{Hz}^{-1}$ ), where  $\langle \Delta p_s^2 \rangle$  represents the mean-square spectral laser power density fluctuation and  $P_{s0}$  the average output power. For convenience the relative noise is described as  $RN = RIN_{laser} / RIN_{pump}$ . Furthermore, the measured system noise ( $RIN_{sys}$ ) includes  $RIN_{laser}$  plus the thermal and shot noise in the receiver.

**Results and discussions:** The parameters used in the calculations are:  $\tau_{21} = 10\text{ms}$ ,  $\sigma_{a,s} = 1.85 \times 10^{-25}\text{m}^2$ ,  $\sigma_{a,p} = 2.08 \times 10^{-25}\text{m}^2$ ,  $\sigma_{e,s} = 3.38 \times 10^{-25}\text{m}^2$ ,  $\sigma_{e,p} = 0.72 \times 10^{-25}\text{m}^2$ ,  $A_{eff} = 12.56\mu\text{m}^2$ ,  $\Gamma_s = 0.77$ ,  $\Gamma_p = 0.79$ ,  $L = 50\text{mm}$ . The coupled-mode calculations use a Bragg grating with coupling coefficient  $\kappa$  and a 4mm long distributed  $\pi$  phase-shift at the grating centre, pump wavelength 1480 nm and lasing wavelength 1560nm. All variables are initialised to the unperturbed steady-state solutions in the calculations.

Fig. 1 shows that the relaxation frequency decreases with higher grating coupling coefficient, which is the same as predicted for DFB semiconductor lasers [3], and also decreases with lower